General Disclaimer

One or more of the Following Statements may affect this Document

- This document has been reproduced from the best copy furnished by the organizational source. It is being released in the interest of making available as much information as possible.

- This document may contain data, which exceeds the sheet parameters. It was furnished in this condition by the organizational source and is the best copy available.

- This document may contain tone-on-tone or color graphs, charts and/or pictures, which have been reproduced in black and white.

- This document is paginated as submitted by the original source.

- Portions of this document are not fully legible due to the historical nature of some of the material. However, it is the best reproduction available from the original submission.

NASA TECHNICAL MEMORANDUM

NASA TM-77503

INFLUENCE OF ALUMINUM OXIDE FILM ON THERMOCOMPRESSION BONDING OF GOLD WIRE TO EVAPORATED ALUMINUM FILM

Seiichi Iwata, Akitoshi Ishizaka, Hiroshi Yamamoto

Translation of Nippon Kinzoku Gakkaishi (Journal of Japan Institute of Metals), Vol. 45, No. 6, 1981, pp. 603-609

NATIONAL AERONAUTICS AND SPACE ADMINISTRATION
WASHINGTON, D.C. 20546 OCTOBER 1984

STANDARD TITLE PAGE

1. Report No. NASA TM-77503	2. Government Accession No.	3. Recipient's Catalog No.
4. Title and Subtitle: INFLUENCE OF ALUMINUM OXIDE FILM ON THERMOCOMPRESSION BONDING OF GOLD WIRE TO EVAPORATED ALUMINUM FILM		5. Report Date: OCTOBER 1984 6. Performing Organization Code
7. Author(s): Seiichi Iwata, Akitoshi Ishizaka, Hiroshi Yamamoto		8. Performing Organization Report No. 10. Work Unit No.
9. Performing Organization Name and Address: Leo Kanner Associates, Redwood City, California 94063		11. Contract or Grant No. NASW-3541 13. Type of Report and Period Covered: Translation
12. Sponsoring Agency Name and Address: NATIONAL AERONAUTICS AND SPACE ADMINISTRATION WASHINGTON, D.C. 20546		14. Sponsoring Agency Code

15. Supplementary Notes

Translation of Nippon Kinzoku Gakkaishi (Journal of Japan Institute of Metals), Vol. 45, No. 6, 1981, pp 603-609

16. Abstract

The influence was studied of Al surface condition on the thermocompression bonding of Au wires to Al electrodes for integrated electric circuits. Au wires were connected to Al electrodes by nail-head bonding after various Al surface treatments. Bonding was evaluated by measureing the wire pull strength and fraction of the number of failures at Au-Al bonds to the total number of failures. Dependence of the fraction on applied load was derived theoretically with a parameter named critical load to take into consideration the difference in Al surface condition. The relation also held explicately for various surface treatments. Characterization of the Al surface was carried out by electron microscopy for chemial analysis.

17. Key Words (Selected by Author(s))	18. Distribution Statement: Unclassified - Unlimited		
19. Security Classif. (of this report): Unclassified	20. Security Classif. (of this page): Unclassified	21. No. of Pages: 25	22. Price

INFLUENCE OF ALUMINUM OXIDE FILM ON THERMOCOMPRESSION BONDING OF GOLD WIRE TO EVAPORATED ALUMINUM FILM

Seiichi Iwata, Akitoshi Ishizaka and Hiroshi Yamamoto

Central Research Laboratory,
Hitachi, Ltd., Kokubunji

1. Introduction

The field of semiconductors has been making remarkable progress recently: very large scale integrated (VLSI) circuits are being developed now in this country as well as abroad. Even when the VLSI era is reached, the need will still exist for bonding semiconductor elements and exterior terminals. Because the number of elements to be bonded is expected to increase in the future [1], we are required to further improve the reliability of bonding of this type.

The process called Au wire thermocompression bonding [2,3] is generally used for the type of bonding mentioned above. Au thin wire of 50-60 μm diameter is used to connect the semiconductor electrodes (this is usually done by evaporation) to external terminals. High speed automated machines became available for this work recently [4], and the technology for bonding has progressed tremendously. However, if the reliability needs to be improved in the future, the bonding defect rate needs to be decreased.

We discussed the faster speed Au wire thermocompression in the previous report [2], in which we reported that the Al

surface condition caused wide dispersion of bondability between Al and Au. This time, we studied how the Al surface affects bondability quantitatively. We first measured Al surface bondability differences when Al is bonded to different specimens, so that we could find out what parameters can express the surface condition differences. This step was based on the theoretical examination. Then, we examined the physical meaning of these parameters, based on the data of the Al surface conditions measured by ESCA (Electron Spectroscopy for Chemical Analysis).

By conducting the studies as discussed above, we were able to clarify quantitatively the effect of Al surface conditions on bondability. We are planning to continue to concentrate our efforts in research so that we can better control the surface condition of evaporated Al.

II Experimental Method

In order to study the effect of Al surface conditions on bondability, we processed in several different ways the surface of evaporated Al placed on a thermally oxidized Si wafer, then bonded Au wire on Al by thermal compression. We measured the bondability by pulling the wire. We then examined experimentally and theoretically what parameter can express the difference of Al surface conditions.

1. Specimen Manufacturing

One μm thick Al was evaporated on thermally oxidized Si wafers in the 0.1 mPa vacuum. The evaporation speed was 10 nm/s and the substrate temperature was 523K (250 C). After the /604 evaporation, the type of surface treatment, as described in Table 1, was conducted on the Al. Then, the wafer was divided into approximately 6 mm square chips, bonded eutectically to the lead frame plated by Au, and then Au wire was bonded to Al on a Si chip and lead frame, as shown in Figure 1.

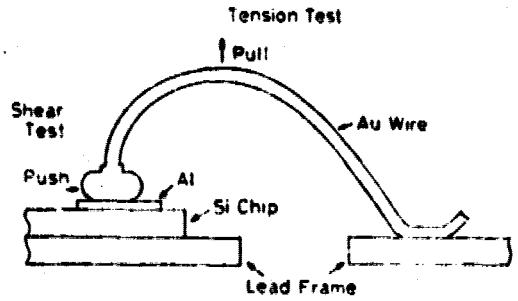

Fig.1 Two methods of testing bond strength.

Table 1 Various surface treatments applied to Al in this study.

Treatment	Condition
Air	293~298 K-604.8 ks (20~25°C-7 d) (~50%R.H.)
Deionized water	293 K-7.2 ks (20°C-2 h)
$HF + NH_4F$ (1 : 6)	293 K-300 s (20°C-5 min)
Deionized water	393-3.6 ks (120°C-1 h)
H_3PO_4	293 K-360 s (20°C-6 min)

2. Bonding Technique and Its Evaluation

We used a computer-aided Au wire compression bonding system (CABS: Computer-Aided Bonding System) manufactured by Hitachi for bonding purposes. The bonding temperature was 573 K (300°C), pressure time 50 ms, and bonding load W was applied up to 0.2-0.8 N.

Tension testing* was conducted in order to examine bondability, as shown in Figure 1. In this testing, the bonded Au wire was pulled upward, and the strength F_T required for breaking the wire off and fraction P of the number of breakages at Au-Al bonds to the total number of breakages were calculated. Incidentally, all breakage occured at the Au-Al junction or in the Au wire (close to the Au-Al junction) in this experiment, but no breakage was observed at the lead frame and Au wire junction.

In this study, we used the ratio of breakage occurring at the bond P as data for evaluating the bondability, because F usually indicates Au wire strength rather than bond strength. (Unless bonding is extremely weak, breakage does not occur at the bond) Even if we decreased the bonding load in order to increase the breakage ratio at the bond, the F_T value dispersion was very large. Furthermore, even if we measured a larger number of F_T's, it would have been very difficult to obtain the true bond breakage force (Refer to Appendix 1). On the other hand, P can be used

---

* Here, the most commonly used tension test is discussed. Another test called the shear test [2], in which bond strength is measured more directly, is discussed in Appendix 2.

in the result analysis as a parameter indicating the amount of bondability, as will be explained in the next chapter. Tension testing was conducted on each group of 300 chips of different bond conditions (of Al surface treatment and bonding load) in order to obtain the P value.

3. Al Surface Condition Measurement

The Al surface was examined by ESCA. A Hitachi E-507 ESCA was used. The vacuum was 0.1 mPa, and an AlK α ray was used for X-ray. Because Al oxide film gives a great effect on bondability as has been reported in the previous paper [2], we measured the peak of the Al2p electron in order to use it as an indication of the oxide film thickness, then obtained the peak strength (hight) ratio between the non-oxide and Al oxide (Figure 3). The thinner the oxide film is, the greater this ratio grows [5]. We defined this ratio as the surface cleanliness scale S. Occasionally, bondability is affected by the amount of C detected on the surface when the Al surface is contaminated by organic materials. But no effect of C was observed in this experiment.

III Result and Examination

In this chapter, the breakage ratio at the bond P will be expressed as a function of the bonding load W. Then, the relation obtained from this and the experimental result will be compared.

In the final step, we will discuss what role the Al surface condition plays in affecting the relation of P and W.

1. The Presumed Effect of Al Surface Condition on Bondability

When the Au ball at the tip of the Au wire is pressed onto the Al surface for bonding, the contact area A_C of Au and Al may be expressed [6]

$$A_C = \frac{W}{\sigma_0} \qquad (1)$$

Here, W represents bonding load, σ_0 the hardness at the bond. If two metals are touching on clean surfaces, the contact area A_B should be equal to A_C. If the surfaces are not clean, $A_B < A_C$ (refer to Appendix 2). Therefore, by applying the amount W_0 in the parameter that expresses the Al surface condition, A_B of the closest primary value can be expressed,

$$A_B = \frac{W - W_0}{\sigma_0} \quad \text{(here, } A_B \geq 0\text{)}. \qquad (2)$$

Next, the relation between the breakage ratio P at the bond and the contact area A_B will be obtained. Because the breakage occurs either at the bond or at the Au wire as has been mentioned, the breakage ratio, when occuring at the Au wire, will be 1-P. Energies required to cause the breakage at the bond and the Au wire are named E_1 and E_2 (per atom), respectively. Then, P can be expressed [7]

$$P = \frac{\exp\left(-\frac{E_1}{kT}\right)}{\exp\left(-\frac{E_1}{kT}\right) + \exp\left(-\frac{E_2}{kT}\right)} \qquad (3)$$

Here, K represents Boltzmann's constant and T, temperature (K).

The breakage at the junction actually occurs in the metal compound grown by the Au and Al bonding reaction. Because the breakage is observed to be of brittle nature, we set the hypothesis that the bond was broken only by elastic deformation. So that we can obtain the energy required for the breakage, we will utilize the distribution of stress and displacement ouccring when a semi-infinite body and a rigid column are put in contact. If we are to consider that the energy required for the breakage equals El, which represents the average energy increase per atom at the circular bond containing N atoms, the following may be established. /605

$$NE_1 = 2 \cdot \frac{1}{2} \int_0^R \sigma_{zz} \cdot U_z \cdot 2\pi r \, dr \qquad (4)$$

The 2 on the right side of this equation is effective because there are two broken sections. σ_{zz} and U_z indicate stress and displacement in the z direction expressed by (r, σ, z) on circular cylindrical coordinates, and R represents the radius of the bond. Furthermore, σ_{zz} and U_z when force F_T is applied may be expressed as follows [8].

$$\sigma_{zz} = \frac{F_T}{2\pi R\sqrt{R^2 - r^2}} \qquad (5)$$

$$U_z = \frac{F_T(1-\nu^2)}{2ER} \qquad (6)$$

Here, F_T represents the energy required for the breakage, and it may be written as

$$F_T = \sigma_T \cdot l_R \qquad (7)$$

and is the bonding strength. E represents Young's modulus and

ν , Poisson's ratio. Neither E nor ν can be given in one specific value in reality, but we did so in order to simplify them.

When Equations 5 and 6 are substituted in Equation 4,

$$NE_1 = \frac{F_T^2(1-\nu^2)}{2ER} \qquad (8)$$

Here,

$$A_B = \pi R^2 \qquad (9)$$

When Equation 7 is substituted in Equation 8,

$$NE_1 = \frac{(\pi R^2 \sigma_T)^2(1-\nu^2)}{2ER} = \frac{\pi^2 \sigma_T^2(1-\nu^2)}{2E} R^3 \qquad (10)$$

Then, when R is expressed as a function of $W-W_0$ by using Equations 9 and 2 and it is substituted in Equation 10,

$$NE_1 = \frac{\sqrt{\pi}\sigma_T^2(1-\nu^2)}{2E\sigma_0^{3/2}} (W-W_0)^{3/2} \qquad (11)$$

Here, if

$$K = \frac{\sqrt{\pi}\sigma_T^2(1-\nu^2)}{2NE\sigma_0^{3/2}} \qquad (12)$$

$$E_1 = K(W-W_0)^{3/2}$$

When Equation 12 is substituted in Equation 3, it will be finally expressed as follows after being organized:

$$kT \ln \frac{1-P}{P} = K(W-W_0)^{3/2} - E_2 \qquad (13)$$

Therefore, if W_0 is a constant, a linear relation will be obtained when log[(1-P)/P] is given to the vertical axis and $(W-W_0)^{3/2}$ to the horizontal axis. We will discuss whether or not the experiment result can be expressed in Equation 13 format in the following chapter.

2. Comparison of Experiment and Theory

First, the surface treatment was conducted on Al specimens,

and Au wire was bonded onto Al with various bonding loads W. Tension testing was conducted then, and the ratio of breakage occurrence at the bond P was computed. Then, we hypothesized that W_0 of Equation 13 was a constant determined by the Al surface condition, and examined whether it was possible to obtain W_0 that may suit Equation 13 in some way. Figure 2 shows the relation between $\log[(1-P)/P]$ and $(W-W_0)^{3/2}$ that was obtained as a result of this effort. This graph shows all the experimental data of the specimens whose surface processings are listed in Table 1. (Approximately 300 data were used to determine each dot.) This graph indicates that the relation between $\log[(1-P)/P]$ and $(W-W_0)^{3/2}$ can be expressed by the same equation by varying W_0. It also indicates that the relation of Equation 13 is established when W is not large. The reason why the relation does not result in a straight line when W is large seems to be because the contact area cannot be set larger than a certain value as the diameter of the Au wire is fixed. The W_0 value for each surface processing established to suit Equation 13 resulted as shown in Table 2. It seems that the reason why we could express the relation between P and W belonging to specimens of different

Table 2 Values of W_0 for various surface treatments.

Treatment	W_0(N)
Air (293~298 K·604.8 ks, ~50%R.H.)	0.02±0.02
Deionized water (293 K·7.2 ks)	0.04
HF + NH_4F (1 : 6, 293 K·300 s)	0.10±0.01
Deionized water (393 K·3.6 ks)	0.4
H_2PO_4 (293 360 s)	0

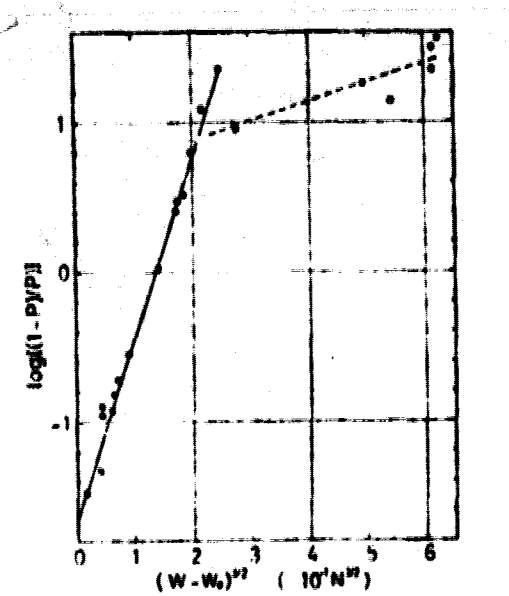

Fig.2 Dependence of fraction P of failures at Au Al bond on applied load W.

surface treatments by only varying the W_0 value, as shown in Figure 2, is because the W_0 value is determined by the difference among /606 Al surface conditions, and each surface treatment gives a fixed value to W_0 even if W is varied. Up to this point, we have discussed the case of tension testing. The W_0 value may be obtained from shear testing also. Refer to Appendix 2 for these data. Next the meaning of W_0 will be discussed. Equation 2 indicates that the contact area A_B becomes smaller with greater W_0, and Equation 3 indicates that there is almost no contact ($P \cong 1$) unless W passes W_0. During the experiment, we also observed that A_B grew smaller when the oxide film on the Al surface was thicker and there was no contact unless we applied a load which was greater than a certain value. We therefore decided to call W_0 a critical load. By using different W_0 values, we can express the effect of Al surface conditions on bondability.

The contaminant attached to the Al surface or oxides generated there seem to cause W_0 to have a great value. Therefore, we investigated the surface conditions of each specimen using an ESCA. No correlation was found to exist between the oxidation degree on the surface and W_0, while some correlation was recognized between the Al oxidation degree and W_0 value. We obtained the peak height ratio between the non-oxide and oxide Al's at the Al2p peak measured by ESCA, and we defined this ratio as surface cleanliness S, which expresses the oxidation degree. The S value is greatly affected by the thickness of the oxide film. The oxide film grows thicker as S is smaller in the closest primary value, although this varies according to different kinds of film. Figure 4 shows the relation between W and W_0. From this diagram, it is clear that W_0 is greater when S is small, which means that the oxide film is thicker. Therefore, if the S value is known, bondability can be predicted. The correlation shown in Figure 4 seems fairly good, but still some deviation is observed. Probably the data of the S values is not sufficient to do an examination in detail and we will need some more information on the type (chemical combination) of the film. This information is thought to be able to be obtained by measuring chemical shift*, but the Al oxide type insulator will be affected by X-radiation during measuring and will charge with electricity even if it is several nanometers thin [9]. Therefore, we are conducting studies so that we can obtain the chemical shift value (determined by the chemical combination) that is not affected by the charged electricity [9]-[11].

In reality (semiconductor element manufacture process), the Al surface is put in contact with $HF+NH_4F$ liquid before bonding. That is when the S value varies in the range of 0.25 to 0.45, the W_0 value varies from 0.05 through 0.13N corresponding to this. The cause of this change is not completely clearly known yet, but it is possible that the Al surface condition changes according to the conditions of water rinsing (although one might think that he is rinsing in the same condition) conducted after surface treatment. Some of the examples are listed in Appendix 3 to describe the effect of water rinsing conducted after surface treatment given to the Al surfaces. Some more studies on $HF+NH_4F$ liquid treatment are planned to be conducted in the future.

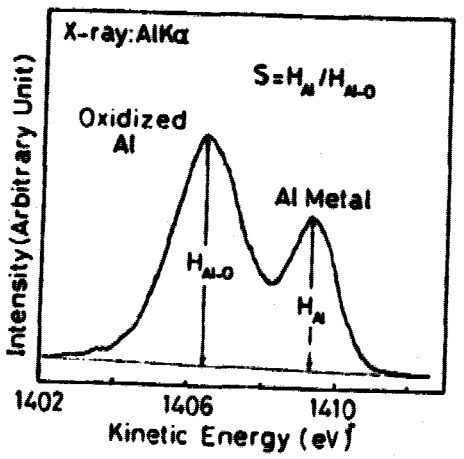

Fig.3 Typical Al2p spectrum obtained in this study.

*This is said to be determined by the Al combination caused by the peak location difference between Al oxide and non-oxide. (Figure 3)

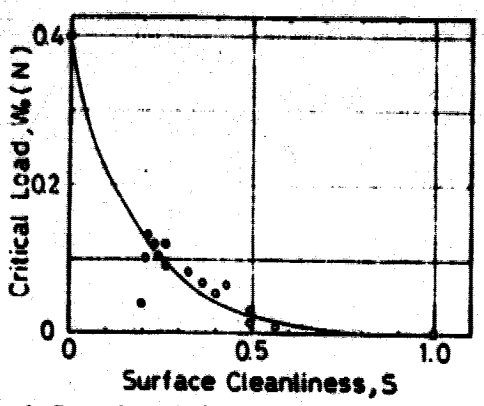

Fig.4 Dependence of critical load W_0 on Al surface cleanliness S(see Fig.3).

IV Conclusion

We examined in this study the effect of Al surface conditions on bondability when Au wire is bonded by thermocompression onto Al evaporation film, and the following result was obtained.

1. When Au wire is pulled, the fraction of the number of failures at Au-Al bonds to the total number of failures P to be used as a measuring scale of bondability can be expressed by

$$kT \ln \frac{1-P}{P} = K(W-W_0)^{3/2} - E_2 \qquad (14)$$

Here, K is a constant determined by the mechanical nature of the bonded part; W, bonding load; E_2 the energy (per atom) required to break the Au wire off; and W_0, a constant (called critical load) determined by the Al surface condition.

2. W_0 grows greater in its closest primary value when the Al oxide film is thicker. And, the W_0 value is able to be estimated by scanning the Al surface by ESCA.

We would like to express our deepest appreciation to

Mr. Michio Tanimoto, Tsutomu Yamasaki of Hitachi Musashino Plant /607
and Motomasa Ogino who has left the Musashino Plant for sharing the work in some of the experiments, to Dr. Kikuji Sato of Hitachi Central Research Center and Dr. Genichi Kamoshita of Hitachi Microcomputer Engineering, Inc. for their efforts to make this research project possible, and to Professor Hideharu Oohara of the Engineering Department of Tohoku University and Professor Shozo Kamoda of the Engineering Department of Hosei University for discussi the experimental result with us.

Appendix

1. The method for computing the breaking force at the bond using the force F_T, a measured value of the force required to break Au wire by pulling [12].

In general when two or more types of breakage coexist, the average breaking force of each breakage type is different from the true average.

When m and n numbers of measured breaking force values are picked from populations B (for example, breakage occurring at the junction) and A (for example, breakage occurring at Au wire) respectively, these values are established as follows:

$$B: x_1, x_2, \cdots\cdots, x_n$$
$$A: y_1, y_2, \cdots\cdots, y_m$$

We define the probability as follows:

$$L=\prod_{i=1}^{n} f_1(x_i)[1-F_2(x_i)]\prod_{j=1}^{m} f_2(y_j)[1-F_1(y_j)] \qquad (15)$$

Here, $f_{1(xi)}$ and $F_{1(xi)}$ are the probability distribution and accumulative distribution function of x_i respectively. Then, if the distribution of the pulling force required to break the bond is normal (when the force is small, the distribution is almost normal, but we do not know what distribution results when the force is great because breakage occurs at Au wire), we can write as follows:

$$f_1(x_i)=\frac{1}{\sqrt{2\pi}\sigma_x}\exp\left(-\frac{(x_i-\mu_x)^2}{2\sigma_x^2}\right) \qquad (16)$$

$$F_1(x_i)=\sum_{k=1}^{i} f_1(x_k) \qquad (17)$$

Here, σ_x and μ_x are the standard deviation and mean value of x_i

respectively. And, $f_{2(yj)}$ and $F_{2(yj)}$ are the probability distribution and accumulative distribution function when breakage occurs at the Au wire.

Using equations 15, 16, 17, we obtain σ_x and μ_x values that are most likely to fit in

$$\frac{\partial L}{\partial \mu_x}=0, \quad \frac{\partial L}{\partial \sigma_x}=0 \tag{18}$$

We estimated the break force at the bond F_{TB} by this method, and the result is listed in Table 3. Thus the average

Table 3 Estimated values of tensile bond breaking force F_{TB} obtained by using most likelihood method.

Applied load (N)	n	m	Measured F_{TB}(N)*	Estimated F_{TB}(N)
0.25	72	42	0.062	0.091
0.40	48	52	0.074	0.11
0.60	12	84	0.085	0.30

* Average of n values of F_{TB}.

value computed from the measured breaking force is somewhat different from the true value; therefore, it is not appropriate to express bondability by the measured breaking force itself. However, there is no need to have such concerns with the breaking force obtained by shearing, because all breakage occurs at the bond.

2. The effect of Al surface condition in shearing testing

In the shearing test, force is applied differently from the tension testing. It is applied from the side onto the bond

(Figure 1), as was discussed in the previous report [2], and the force required to break the junction is measured. Therefore this breaking force indicates the strength of the bond itself. We thus utilized a bond breaking force F_s that was measured and the scale indicating the Al surface condition. The relation between the bond breaking force and surface cleanliness S can be obtained directly without any computation. Figure 5 shows the relation between the bond breaking force F_s and the surface condition of Al-Mn evaporation film [13] which we developped to use as anti-corrosion wiring material. We conducted this testing because Al-Mn material does not have as good bondability as Al although it is more anti-corrosive than Al. Each dot in Figure 5

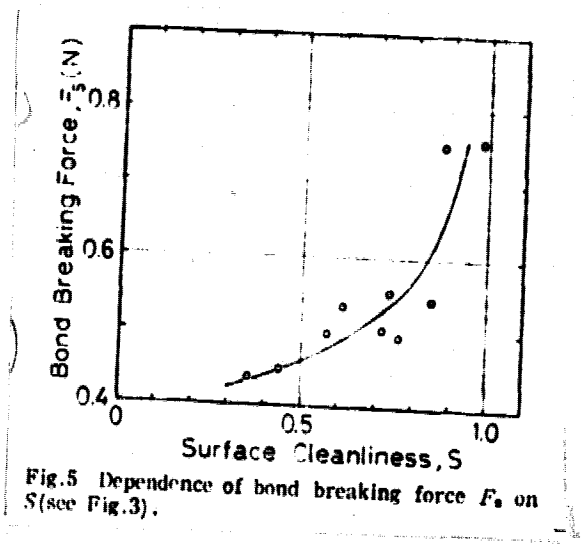

Fig.5 Dependence of bond breaking force F_s on S(see Fig.3).

indicating a F_s value is an average of 40 breaking force measurements.

In order to correspond this testing and tension testing, Fs was expressed as a function of bonding load W. Figure 6 shows a

photograph of the typical look of the piece broken in a shearing test and the method for measuring the apparent contact area and the apparent bond area*. The apparent contact area a_C is defined as

$$a_C = \frac{\pi}{4}\left(\frac{D_{C1}+D_{C2}}{2}\right)^2 \tag{19}$$

and the apparent contact area a_B is defined as

$$a_B = \frac{\pi}{4}\left(\frac{D_{B1}+D_{B2}}{2}\right)^2 \tag{20}$$

The average of 40 measurements was used as the value of each diameter.

Figure 7 shows a_C dependency on W. As is clear from this diagram, the relationship discussed above can be drawn by straight line and it can be expressed as follows.

$$a_C = \frac{W}{\sigma_0'} + a_0 \tag{21}$$

Here, 185 MPa is given as the σ_0' value in Figure 7. This is almost

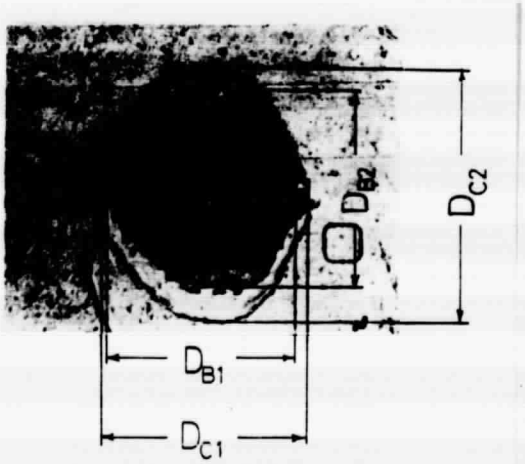

$$a_B = \frac{\pi}{4}\left(\frac{D_{B1}+D_{B2}}{2}\right)^2$$

$$a_C = \frac{\pi}{4}\left(\frac{D_{C1}+D_{C2}}{2}\right)^2$$

Fig.6 Method of obtaining apparent bond area a_B and apparent contact area a_C.

*This is the area where the Au-Al compound is generated by the bonding reaction.

equal to the hardness that was measured at 573K (bonding temperature). When two lumps are put in contact, σ_0 should indicate the hardness of the softer lump, but it indicates Au hardness rather than Al in tnis testing. It seems that hardness of SiO_2 and Si under Al gave some effect because Al was only 1 μm thick (both SiO_2 and Si are harder than Au).

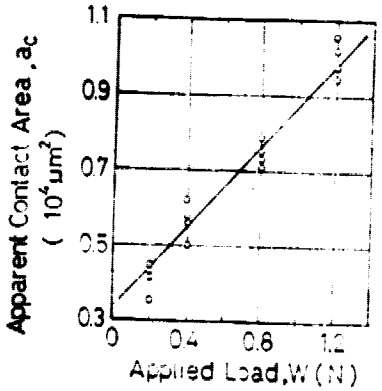

Fig.7 Dependence of apparent contact area a_c on applied load W.

The following definitions are established after comparing this case with the tension testing.

$$a_B = \frac{W - W_0}{\sigma_0} + a_0 \qquad (22)$$

$$F_s = \tau a_B \qquad (23)$$

Here, W_0 is the critical load defined in chapter III-1, and is an apparent shearing breaking force. Thus Equation 22 can be substituted in equation 23.

$$F_s = \tau\left(\frac{W - W_0}{\sigma_0} + a_0\right) \qquad (24)$$

We obtained the equation that expresses the relation of Fs and W as indicated in Figure 8. Therefore, the following two equations can be used for computing W_0 from the shearing test.

$$a_C - a_B = \frac{W_0}{\sigma_0} \qquad (25)$$

$$\Delta F_s = -\frac{\tau}{\sigma_0}\Delta W_0 \qquad (26)$$

Here, ΔF_s and ΔW_0 represent differences between two F_s's or W_0's. W_0 can be obtained from Equation 25 directly. Or if one W_0 is known, another W_0 can be obtained by substituting the F_s change in Equation 26. Here, we obtained a W_0 value of two surface treatments by using Equation 25. The result is shown in Table 4. The W_0 obtained here corresponds well with the W_0 obtained from tension testing.

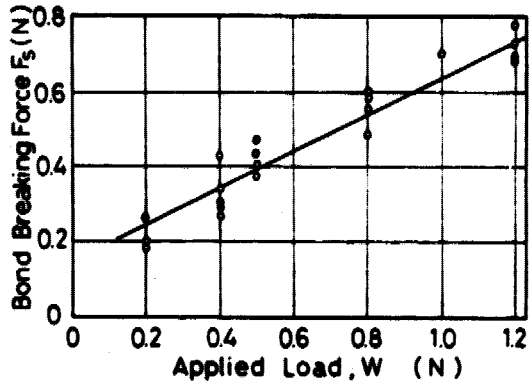

Fig.8 Dependence of bond breaking force F_s on applied load W.

Table 4 W_0 obtained from shear test.

Surface treatment	W_0(N)
$HF+NH_4F$ (1 : 6, 293 K-300 s)	0.13±0.06
Air (293~298 K-604.8 ks, ~50%R.H.)	0.02±0.02

3. The effect of a water rinse performed after Al surface treatment on Al surface condition

In chapter III, we discussed the possibility of a water rinse performed after Al surface treatment changing the thickness

of the Al oxide film. Here, we will discuss the case where an oxide film thickness actually changed because of different water rinse conditions. The Al evaporation film contained 2 mass% Mn in this case.

As has been mentioned, Al-Mn evaporation film is superior in anti-corrosiveness to Al film, but it does not have as good bondability. Therefore, surface treatment for thinning the oxide film is required when this type of film is used. By conducting sulfamine acid treatment (5 mass% solution, 333K-900s (60 C-15 min)), Al level bondability can be obtained with Al-Mn film. However, a large amount of dispersion was observed in bondability when this was actually performed. We studied the relation between bondability and Al-Mn surface condition in order to clarify the cause of dispersion, and we found that there was a correlation between surface cleanliness S and breaking force, just as in the case of Al film (Figure 5). Furthermore, even if the same sulfamine acid treatment is performed, the S value may vary depending upon the water rinse conducted after the treatment, as shown in Figure 9. Here, the water rinse condition

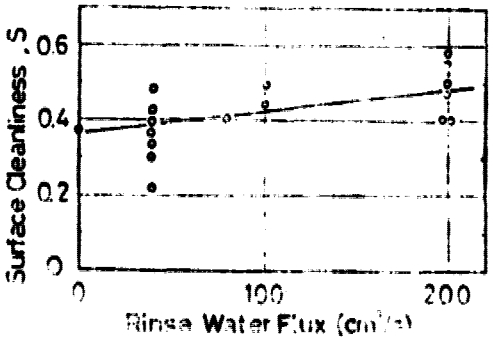

Fig.9 Dependence of Al surface cleanliness *S* on rinsing condition after sulfamic acid surface treatment.

is indicated by the amount of pure water run per unit time used for rinsing. An Si wafer evaporated with Al-Mn film was rinsed in a 500 cm^3 beaker under a faucet of pure water.

BIBLIOGRAPHY

1. Keyes, R. W., IEEE J. Sol.-St. Circ., SC-14 (1979), 193
2. Iwata, S., Ishizaka, A., Yamamoto, H., Nippon Kinzoku Gakkaishi (J. Japan Inst. Metals.) 41(1977), 1154.
3. Iwata, S., Ishizaka, A., Yamamoto, H., Nippon Kinzoku Gakkaishi 41(1977) 1154.
4. Iwata, S., Ishizaka, A., Yamamoto, H., Nippon Denshi Zairyo Gijutsu Hokoku (J. Japanese Electronic Material Technology) 10(1979) 12.
5. Ishizaka, A., Iwata, S, Kamigaki, Y., Surf. Sci., 84(1979), 12.
6. Cottrell, A.H., The Mechanical Properties of Matter, John Wiley and Sons, Inc., New York, (1964), 332.
7. Kittel, C., Elementary Statistical Physics, John Wiley and Sons, Inc., New York, (1958), 54.
8. Timoshenko, S., Theory of Elasticity, McGRaw Hill Book Co., New York, (1934), 338.
9. Iwata, S., Ishizaka, A., Nippon Kinzoku Gakkai Shi, 42(1978), 1021.
10. Iwata, S., Ishizaka, A., Nippon Kinzoku Gakkai Shi, 43(1979), 380.
11. Iwata, S., Ishizaka, A., Nippon Kinzoku Gakkai Shi, 43(1979), 388.
12. Kamota, S., Iwata, S., Ooyo Tokeigaku (Applied Statistics), 5(1977), 63.
13. Iwata, S., Ishizaka, A., Yamamoto, H., J. Electrochem. Soc., 126(1979), 110.